# Calcium influx is sufficient to induce muscular dystrophy through a TRPC-dependent mechanism

Douglas P. Millay[a], Sanjeewa A. Goonasekera[a], Michelle A. Sargent[a], Marjorie Maillet[a], Bruce J. Aronow[a], and Jeffery D. Molkentin[a,b,1]

[a]Department of Pediatrics, Cincinnati Children's Hospital Medical Center, and [b]Howard Hughes Medical Institute, University of Cincinnati, Cincinnati, OH 45229

Edited by Eric N. Olson, University of Texas Southwestern Medical Center, Dallas, TX, and approved September 16, 2009 (received for review June 12, 2009)

**Muscular dystrophy is a general term encompassing muscle disorders that cause weakness and wasting, typically leading to premature death. Membrane instability, as a result of a genetic disruption within the dystrophin-glycoprotein complex (DGC), is thought to induce myofiber degeneration, although the downstream mechanism whereby membrane fragility leads to disease remains controversial. One potential mechanism that has yet to be definitively proven in vivo is that unregulated calcium influx initiates disease in dystrophic myofibers. Here we demonstrate that calcium itself is sufficient to cause a dystrophic phenotype in skeletal muscle independent of membrane fragility. For example, overexpression of transient receptor potential canonical 3 (TRPC3) and the associated increase in calcium influx resulted in a phenotype of muscular dystrophy nearly identical to that observed in DGC-lacking dystrophic disease models, including a highly similar molecular signature of gene expression changes. Furthermore, transgene-mediated inhibition of TRPC channels in mice dramatically reduced calcium influx and dystrophic disease manifestations associated with the *mdx* mutation (dystrophin gene) and deletion of the δ-sarcoglycan (*Scgd*) gene. These results demonstrate that calcium itself is sufficient to induce muscular dystrophy in vivo, and that TRPC channels are key disease initiators downstream of the unstable membrane that characterizes many types of muscular dystrophy.**

fibrosis | necrosis | degeneration | skeletal muscle

A number of diverse genetic mutations result in muscular dystrophy (MD), although most occur in proteins that either reside within or are associated with the dystrophin-glycoprotein complex (DGC) (1). For example, mutations in the dystrophin gene in Duchenne or Becker MD or mutations in any one of the sarcoglycans can cause destabilization of the muscle cell membrane and a dystrophic phenotype (1, 2). The DGC is a large protein complex that spans the sarolemma and affixes the basal lamina outside the cell to the contractile proteins within the cell and when defective, can lead to membrane damage after contraction (3, 4). A defect in the stability of the sarcolemma is widely accepted as the initiating stimulus underlying most forms of MD, although the next step in the process leading to myofiber degeneration has long been debated. One long-standing hypothesis is that defects in the membrane permit calcium entry (5, 6), thus activating calpains and/or mitochondrial swelling (7–9). However, that intracellular calcium levels are elevated in dystrophic fibers, or even within the subsarcolemmal space, remains unproven and controversial (10–14). Another point of contention relating to the calcium hypothesis, is the route of entry. Whether calcium enters through ''microtears'' in the sarcolemma, or by a more active process involving ion channels remains to be resolved. Indeed, calcium leak channels, stretch-activated channels, receptor-operated channels, and store-operated calcium channels have been implicated as calcium influx pathways in MD (15–18). While the identity of these putative channels has been elusive, the transient receptor potential canonical (TRPC) family of nonselective cation channels has been proposed. However, it remains unknown if unregulated calcium influx truly initiates/mediates myofiber degeneration in MD, nor has definitive proof emerged implicating TRPC channels as mediators of this disease in vivo.

## Results

**Generation of TRPC3 Skeletal Muscle-Specific TG Mice.** Here we generated transgenic mice with TRPC3 overexpression specifically in skeletal muscle using the skeletal α-actin promoter as a means of elevating calcium influx (Fig. 1*A*). Multiple founder lines were generated and one was selected for analysis that showed approximately 6-fold TRPC3 protein overexpression in skeletal muscle, but not in other organs or tissues (Fig. 1*B*). Immunohistochemistry from quadriceps of TRPC3 transgenic mice confirmed that the overexpressed protein was appropriately localized to the sarcolemma, similar to endogenous TRPC3 in wild-type (WT) muscle (Fig. 1*C*). To directly assess TRPC3 activity we measured calcium entry after store depletion in flexor digitorum brevis (FDB) fibers from 2-month-old WT and TRPC3 TG mice. Fura-2 loaded fibers were first perfused with calcium-free buffer, and then treated with EGTA and CPA (SERCA inhibitor) to deplete intracellular calcium over several minutes. Caffeine was also applied to further ensure store depletion. The perfusate was changed to a buffer again containing calcium so that store-operated calcium entry (SOCE) could be monitored. A relatively small amount of SOCE was detectable in all WT fibers (Fig. 1 *D* and *F*). In contrast, FDB fibers from TRPC3 TG mice exhibited a dramatic enhancement in SOCE (Fig. 1 *E* and *F*). These results demonstrate the successful generation of transgenic mice with enhanced TRPC3-dependent calcium entry in skeletal muscle.

**TRPC3 TG Mice Develop Severe MD-Like Disease.** MD has been associated with increased expression and activation of TRPC channels in cultured myofibers or myotubes (18–21), although their potential role in vivo as disease mediators has never been examined. Remarkably, TRPC3 TG mice showed profound wasting of all skeletal muscles examined at 2 months of age by direct measurement of muscle weights (Fig. 2*A*), reminiscent of the type of MD observed in *Lama2*$^{-/-}$ mice that also lack a pseudohypertrophy phase. However, the soleus muscle showed a mild pseudohypertrophy phase at 2 months of age that was eventually lost by 6 months of age (Fig. 2 *A* and *B*). By 6 months of age all other skeletal muscles examined showed even more wasting, while the heart was unaffected (Fig. 2*B*). Histological analysis of muscle from TRPC3 TG mice showed profound disease at 2 months of age, characterized by increased central nucleation of fibers (due to degeneration/regeneration cycles), increased numbers of smaller myofibers, fibrosis, and infiltration of inflammatory cells (Fig. 2 *C*, *E*, and *F*,

Author contributions: D.P.M. and J.D.M. designed research; D.P.M., S.A.G., M.A.S., and M.M. performed research; B.J.A. analyzed data; and D.P.M. and J.D.M. wrote the paper.

The authors declare no conflict of interest.

This article is a PNAS Direct Submission.

[1]To whom correspondence should be addressed. E-mail: jeff.molkentin@cchmc.org.

This article contains supporting information online at www.pnas.org/cgi/content/full/0906591106/DCSupplemental.

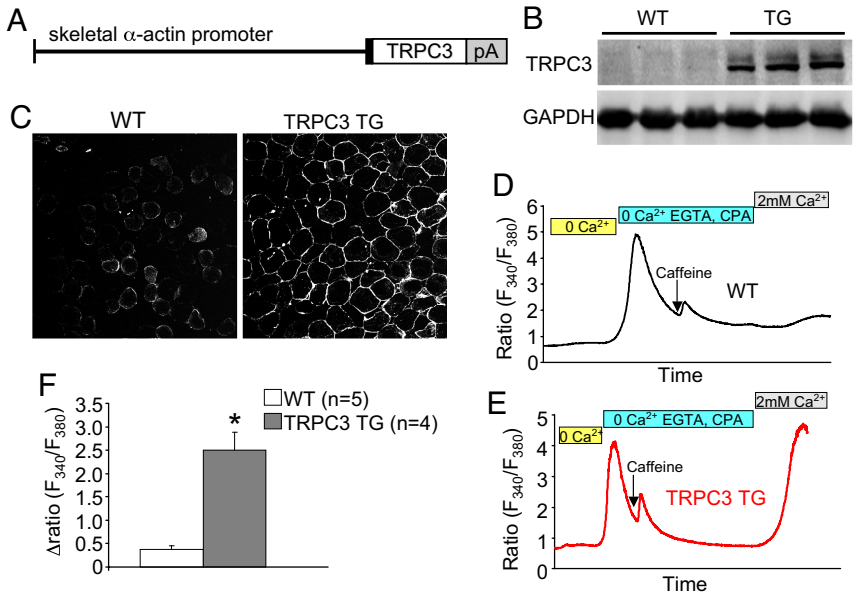


**Fig. 1.** TRPC3 transgenesis enhances calcium influx. (*A*) Schematic of the construct used to make TRPC3 TG mice. pA represents polyA sequence. (*B*) Western blotting for TRPC3 protein in wild-type (WT) and TRPC3 TG mice from quadriceps at 2 months of age. GAPDH was used as a loading control. (*C*) Immunohistochemistry showing TRPC3 localization to the sarcolemma in WT and TRPC3 TG quadriceps. (*D* and *E*) A representative trace of fura-2 fluoresence ($F_{340}/F_{380}$) for store-operated calcium entry (SOCE) from a WT or TRPC3 TG FDB myofiber. The bars above the tracings show the different perfusates that were used in the 3-different stages (see *Methods*). (*F*) Quantitation of fura-2 ratio changes in WT and TRPC3 TG myofibers from a total of 5 WT and 4 TRPC3 TG mice were assayed (5–10 fibers analyzed per mouse). *, $P < 0.05$ vs. WT.

and see Fig. S1 *A* and *B*). By 6 months of age histological analysis showed even more disease characterized by fatty tissue replacement throughout the muscle, increased fibrosis, greater variations in fiber area distributions, and prominent macrophage infiltration (Fig. 2*D* and Fig. S1 *C–F*). All these features suggest that TRPC3 overexpression induces dystrophy and not myopathy, although we also

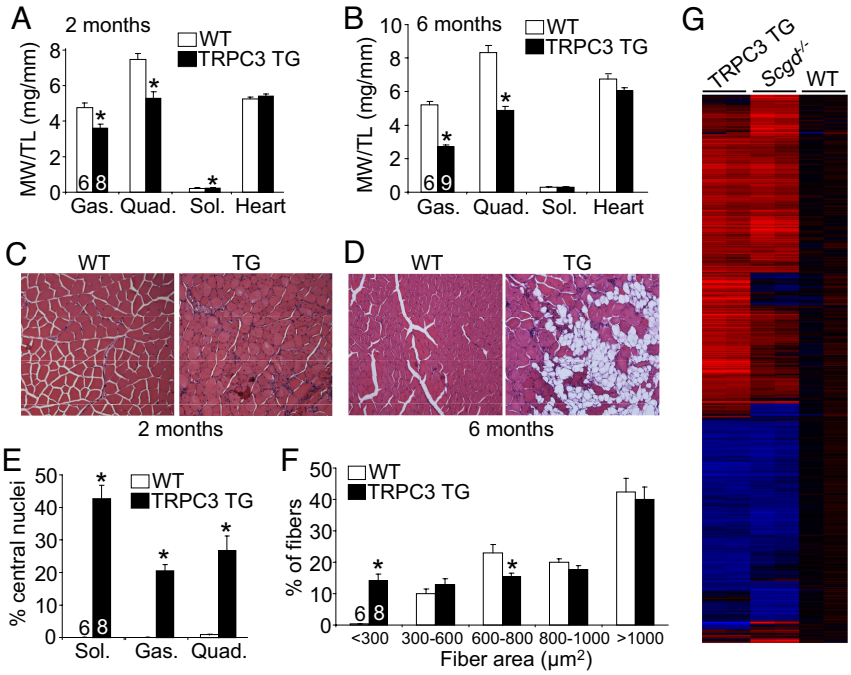


**Fig. 2.** TRPC3-dependent calcium influx induces MD-like disease. (*A* and *B*) Muscle weights normalized to tibia length from the gastrocnemius (Gas.), quadriceps (Quad.), soleus (sol.), and heart in WT and TRPC3 TG mice at 2 and 6 months of age. *, $P < 0.05$ versus WT. Number of mice analyzed is shown in the bars. (*C* and *D*) H&E-stained sections of the quadriceps from 2- and 6-month-old WT and TRPC3 TG mice. Images are shown at 400× magnification. (*E*) Quantitation of the percent of fibers containing central nuclei in the soleus, gastrocnemius, and quadriceps from 2-month-old mice. *, $P < 0.05$ versus WT. Six WT mice were compared against eight TG mice. (*F*) Fiber areas from quadriceps of WT and TRPC3 TG mice separated into ranges. *, $P < 0.05$ versus WT. Six WT mice were compared against eight TG mice. (*G*) Heat map of significant mRNA changes organized in clusters from skeletal muscle of the indicated mice in duplicate. Blue represents downregulated genes from WT control and red are upregulated genes.

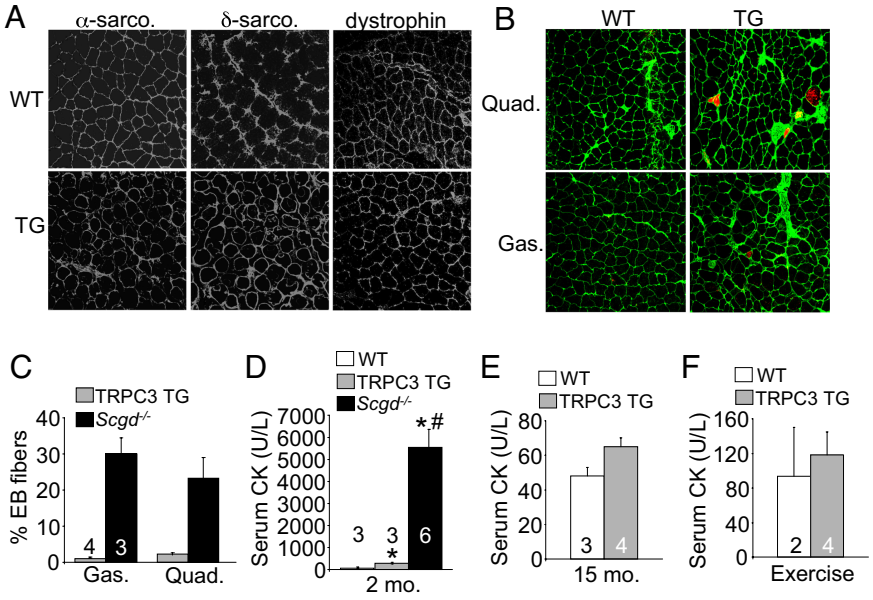


**Fig. 3.** Membrane leakiness is minimal in TRPC3 TG myofibers. (*A*) Immunohistochemistry for δ-sarcoglycan, α-sarcoglycan, and dystrophin in WT and TRPC3 TG quadriceps. Four mice per genotype were analyzed where 400× magnification is shown. (*B*) Evan's blue dye (EBD) uptake after exercise shown as red fluorescence from WT and TRPC3 TG gastrocnemius and quadriceps. Membranes are stained in green with wheat germ agglutinin conjugated to FITC where 400× magnification is shown. (*C*) Quantitation of EBD uptake in muscle from TRPC3 TG and $Scgd^{-/-}$ mice. Four mice were analyzed for each group of mice. EBD myofibers were not observed in WT mice. (*D*) Quantitation of serum creatine kinase (CK) in WT, TRPC3 TG and $Scgd^{-/-}$ mice at 2 months of age. *, $P < 0.05$ versus WT; #$P < 0.05$ versus TRPC3 TG. Number of mice analyzed is shown in the graph. (*E*) CK serum levels in the indicated groups of mice at 15 months of age. (*F*) CK serum levels in 2-month-old mice after voluntary wheel running.

performed mRNA profiling to further compare the molecular signature of disease with an established mouse model of MD due to deletion of δ-sarcoglycan ($Scgd^{-/-}$). Remarkably, of the approximately 3,100 mRNAs that were significantly changed from WT values in skeletal muscle from $Scgd^{-/-}$ mice, the vast majority were similarly altered in TRPC3 transgenic mice, with the same general pattern of altered gene clusters (Fig. 2*G*). Taken together these results indicate that TRPC3 overexpression and the resultant increase in calcium influx directly induces a dystrophic phenotype in skeletal muscle.

**Dystrophic Disease in TRPC3 TG Mice Is Not Due to an Unstable Sarcolemma.** Many genetic mutations that result in MD directly or indirectly impact the stability of the sarcolemma with loss of DGC components. However, immunohistological analysis of skeletal muscle from TRPC3 TG mice and WT controls showed no loss of DGC protein components from the membrane, such as α-sarcoglycan, δ-sarcoglycan, and dystrophin (Fig. 3*A*). Evans blue dye (EBD) uptake, a measurement of membrane tears in vivo, was only minimally increased in TRPC3 TG mice after exercise, despite massive ongoing myofiber degeneration (Fig. 3 *B* and *C*). To put these observations into perspective, $Scgd^{-/-}$ mice were used given their known uptake of EBD throughout affected muscles (Fig. 3*C*). These results suggest that the minor EBD uptake observed in TRPC3 TG muscle is marking necrotic fibers, while EBD positivity in $Scgd^{-/-}$ mice likely represents mostly transient ongoing membrane ruptures in non-necrotic fibers. Indeed, assessment of myofiber membrane rupture by quantifying serum creatine kinase (CK) levels showed only minimal increases in TRPC3 TG mice compared with robust increases in $Scgd^{-/-}$ mice (Fig. 3*D*). Even at 15 months of age, CK release remained relatively unaffected in TRPC3 TG mice (Fig. 3*E*). More importantly, 2-month-old TRPC3 mice subjected to exercise stimulation to enhance membrane stress also showed no increase in CK release (Fig. 3*F*). These results indicate that TRPC3 overexpression generates dystrophic disease without major changes in sarcolemma stability.

**Generation of Transgenic Mice with Inhibited TRPC Activity.** While TRPC channels have been implicated as mediators of unregulated calcium influx in dystrophic myofibers or myotubes in culture, their causative role in mediating disease in vivo is unknown. To address this shortcoming we generated TG mice that overexpress a dominant negative (dn) mutant of TRPC6 using the same skeletal α-actin promoter (Fig. 4*A*). TRPC channels form hetero-tetramers in vivo so that overexpression of a nonconducting mutant channel can disrupt the activity of endogenous channel complexes. Western blot analysis demonstrated protein overexpression in all skeletal muscles examined from the transgene (Fig. 4*B*), which did not negatively impact the development or health of skeletal muscle as assessed by histological methods (Fig. S2*A*). To ascertain the effectiveness of the dnTRPC6 transgene in antagonizing TRPC-dependent calcium influx we crossed these mice with TRPC3 overexpressing transgenic mice. The dnTRPC6 transgene significantly attenuated all aspects of disease associated with TRPC3 overexpression, such as histopathology, the increase in number of smaller fibers, and the number of myofibers with central nucleation (Fig. S2 *B–D*). Importantly, crossing the dnTRPC6 and TRPC3 transgenes did not result in promoter competition, as disease inducing TRPC3 protein levels remained constant (Fig. S2*E*). Collectively, these results indicate that the dnTRPC6 transgene effectively antagonizes the activity and disease causing aspects of TRPC channels in skeletal muscle.

The dnTRPC6 transgene also blocked the increase in SOCE that typifies dystrophic myofibers. FDB myofibers were isolated from WT, dnTRPC6, $Scgd^{-/-}$, and $Scgd^{-/-}$ dnTRPC6 mice for analysis of SOCE as described earlier. While the dnTRPC6 transgene did not demonstrate reductions in baseline SOCE in WT fibers, mostly for sensitivity reasons, it did block the increase in SOCE from FDB fibers of $Scgd^{-/-}$ mice (Fig. 4 *C–G*). These

CELL BIOLOGY

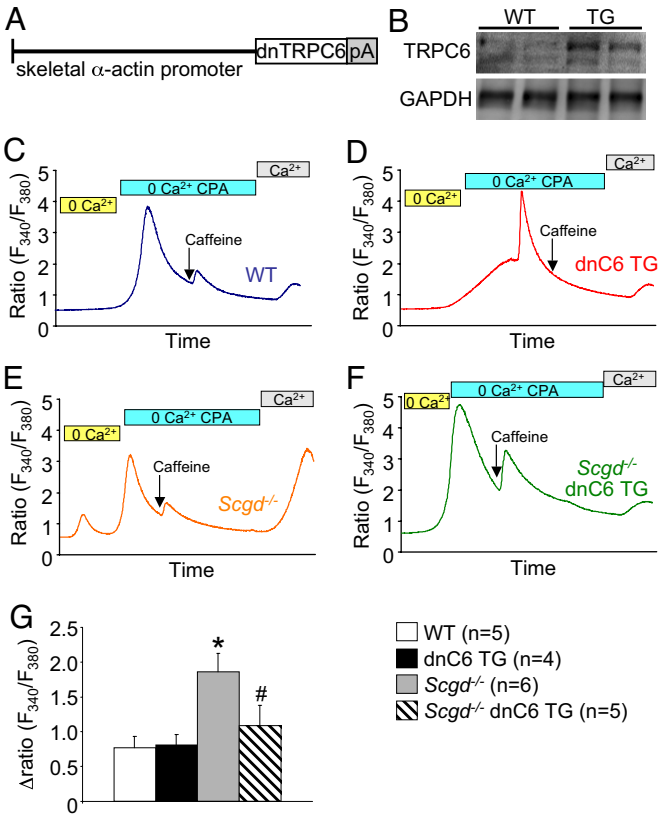


**Fig. 4.** SOCE in dystrophic fibers is reduced by inhibition of TRPC activity (*A*) schematic representation of the dnTRPC6 transgene. (*B*) Western blot for expression of the dnTRPC6 protein in quadriceps from WT and TG mice. (*C*) Representative fura-2 tracings from a single WT FDB myofiber subjected to the buffer conditions shown while simultaneously measuring fluorescence. (*D–F*) Representative fura-2 tracings from a single dnTRPC6, *Scgd*$^{-/-}$, or double *Scgd*$^{-/-}$ dnTRPC6 FDB myofiber subjected to the buffer conditions shown while simultaneously measuring fluorescence (*G*) Quantitation of multiple tracings from the indicated groups for SOCE as a change in the fura-2 fluorescence ratio. The number of mice used is shown, and 5–8 fibers were analyzed per mouse. *, $P < 0.05$ vs. Wt and dnTRPC6 Tg. #$P < 0.05$ vs. TRPC3 TG.

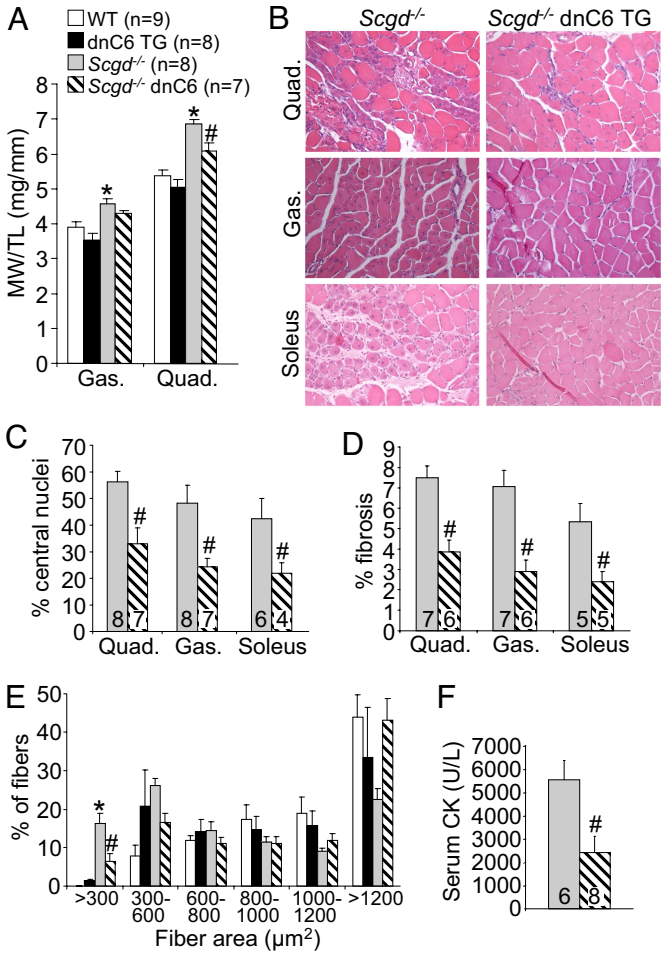


**Fig. 5.** Inhibition of TRPC channels reduces disease in *Scgd*$^{-/-}$ mice. (*A*) Muscle weights normalized to tibia length at 6 weeks of age in the indicated groups of mice from the gastrocnemius and quadriceps. The legend in this panel applies to the remainder of the panels. (*B*) H&E-stained histological sections from *Scgd*$^{-/-}$ and double *Scgd*$^{-/-}$ dnTRPC6 mice from quadriceps, gastrocnemius, and soleus. (400× magnification) (*C*) Quantitation of myofibers with central nuclei in quadriceps, gastrocnemius, and soleus of the indicated groups of mice. #$P < 0.05$ versus *Scgd*$^{-/-}$. (*D*) Quantitation of fibrotic area by Masson's trichrome staining from histological sections in *Scgd*$^{-/-}$ and double *Scgd*$^{-/-}$ dnTRPC6 mice. #$P < 0.05$ versus *Scgd*$^{-/-}$. (*E*) Quantitation of fiber area distributions in all 4 groups of mice. *, $P < 0.05$ versus WT; #$P < 0.05$ versus *Scgd*$^{-/-}$. (*F*) Serum CK levels in *Scgd*$^{-/-}$ and double *Scgd*$^{-/-}$ dnTRPC6 mice. #$P < 0.05$ versus *Scgd*$^{-/-}$.

results indicate that overexpression of dnTRPC6 can antagonize calcium current changes that occur in dystrophic myofibers.

**Inhibition of Endogenous TRPC Channels Attenuates MD.** Given that dnTRPC6 blocked the increase in SOCE that occurs in dystrophic myofibers of *Scgd*$^{-/-}$ mice, we next carefully examined the potential effects on disease progression in the *mdx* and *Scgd*$^{-/-}$ MD mouse models. Analysis of muscle weights showed a significant reduction in pseudohypertrophy in the quadriceps of *Scgd*$^{-/-}$ dnTRPC6 TG mice compared with *Scgd*$^{-/-}$ mice alone at 2 months of age (Fig. 5*A*). Histopathology in *Scgd*$^{-/-}$ mice was also remarkably improved by the presence of the dnTRPC6 TG in all muscles examined (Fig. 5*B*). Specifically, quantitation of myofibers with central nuclei, total area of fibrosis, number of small fibers, and serum CK levels were all significantly reduced by the dnTRPC6 transgene compared with *Scgd*$^{-/-}$ mice alone (Fig. 5 *C–F*). Finally, most of the gene alterations observed in *Scgd*$^{-/-}$ skeletal muscle were reversed with the dnTRPC6 transgene in the Affymetrix array study shown in Fig. 2*G*.

A similar analysis was performed in *mdx* mice, which also showed improved dystrophic disease with the dnTRPC6 transgene (Fig. S3*A*). For example, histological examination of disease in skeletal muscle showed less central nuclei, less small fibers, and less fibrosis in *mdx* mice containing the dnTRPC6 TG (Fig. S3 *B–D*). Total CK release was also reduced by the dnTRPC6 transgene in the *mdx* background compared with *mdx* alone (Fig. S3*E*). Taken together, these results indicate that TRPC channels are important disease determinants in two defined mouse models of MD, suggesting a therapeutic vantage point.

## Discussion

Total intracellular calcium concentration in skeletal muscle cells isolated from dystrophic mice or humans was reported as significantly increased (6), although later studies failed to confirm these results (10, 12, 14, 22). A similar controversy persists as to if subsarcolemmal calcium levels are increased in dystrophic myotubes or myofibers (11, 13). Thus, the original hypothesis that calcium itself can promote MD by inducing myofiber necrosis, which was proposed more than two decades ago, has yet to be definitively evaluated in vivo. Here we showed that overexpression of TRPC3 was sufficient to induce disease se-

quelae that models common forms of MD, such as observed in humans or mice lacking components of the DGC. The phenotype associated with TRPC3 overexpression most closely resembles a dystrophy, not a myopathy, given the observation of fibrosis, fatty tissue replacement, degeneration of myofibers followed by cycles of regeneration, and infiltration of immune cells. The molecular signature of gene expression changes in diseased TRPC3 skeletal muscle is also highly similar to that observed in *Scgd*$^{-/-}$ mice. Thus, these results demonstrate that MD can be initiated by a calcium-dependent mechanism in vivo (i.e., that calcium is a second messenger for disease).

Dystrophic skeletal myofibers are more prone to "microtears" in the sarcolemmal leading to passive calcium entry through physical openings. For example, myofibers from *mdx* mice were shown to be more susceptible to contraction- or stress-induced calcium influx, suggesting a physical discontinuity of the sarcolemma as a primary mechanism (4, 23). These results are also supported by the very basic observation that dystrophic skeletal myofibers leak CK out, and that membrane-impermeable dyes have access in (24). Indeed, the body of work on dysferlin deficiency in MD (dysferlin is a calcium-activated repair protein) suggests that simply diminishing membrane repair capacity of a skeletal myofiber leads to MD disease, presumably due to increased calcium influx (25, 27). In contrast to the membrane rupture hypothesis, direct measurements of membrane currents showed that dystrophic myofibers have increased calcium leak across channels (16), and while the identity of these channels remains elusive, TRPC channels have been proposed (17, 19). Skeletal muscle fibers or myotubes also show SOCE or capacitative calcium entry, which is easily measured after the SR has been depleted of calcium (28–31), although the molecular components responsible for this type of calcium entry in skeletal muscle is still a matter of debate (32).

TRPC1, 3, 4, 5, and 6 are each expressed in skeletal muscle (18), of which TRPC1 and TRPC3 are upregulated in MD (18, 20, 33). TRPC channels have been previously implicated in calcium entry associated with MD using mostly in vitro approaches. For example, antisense based inhibition of TRPC1, 4, and 6 reduced calcium leak activity in dystrophic skeletal myofibers in culture by 90%, strongly suggesting that TRPC channels play a role in calcium leak in MD (18). Other data generated with nonselective inhibitors are supportive, although far from definitive in identifying TRPC channels as the mediators of disease or calcium entry. For example, the rise in intracellular calcium after stretching skeletal myofibers from *mdx* mice was prevented with gadolinium, streptomycin, or the spider venom inhibitor GsMTx4 (21). Interestingly, treatment of *mdx* mice with streptomycin (streptomycin has mild inhibitory activity on store-operated calcium entry) for 2 weeks reduced the uptake of a membrane-impermeable dye in skeletal myofibers, suggesting less leakiness in vivo (34). Finally, TRPC1 was also reported to directly complex with $\alpha$1-syntrophin and dystrophin in muscle cells, and that disruption of this interaction in *mdx* mice likely promotes enhanced TRPC1 activity (20). More recently, the related TRPV channels were also implicated in MD pathogenesis. TRPV2 was shown to translocate to the membrane in dystrophic fibers and overexpression of dominant negative TRPV2 reduced disease in *mdx* mice (35). However, it is not known if TRPV channels function independent of TRPC channels or form common units that coordinately regulate calcium influx depending on the nature of the stimuli.

TRPC channels are relatively nonselective cation channels that also permit sodium entry (usually equivalent to calcium), which is interesting given a report that sodium levels are nearly 2-fold higher in dystrophic fibers from *mdx* mice (36). Elevated sodium levels, while not directly disease-inducing, can secondarily increase calcium by a mechanism involving reverse mode calcium entry through the sodium/calcium exchanger (NCX) (37). For example, increased NCX reverse mode current was detected in human myotubes from Duchenne MD patients (38). More recent data even suggest that greater $Na_v1.4$ activity in MD fibers causes large sodium elevations that are associated with cell death (39). Thus, overexpression of TRPC3 likely mimics the known physiologic profile of ion handling disturbances in MD, such that increases in sodium would further enhance calcium and its primary disease inducing activities. Increased calcium would then activate the intracellular protease calpain, which is known to underlie myofiber necrosis in MD (8, 9), as well as induce mitochondrial swelling and rupture through a separate mechanism (7).

In summary, we propose a model of calcium entry in dystrophic fibers that begins with genetic loss of a member of the DGC, leading to secondary influx of calcium through TRPC channels to promote myofiber degeneration. We also present evidence for the hypothesis that calcium is the secondary messenger for myofiber degeneration common to many forms of MD. These results suggest that inhibitors against TRPC channels would be a therapeutic strategy for treating diverse forms of MD.

## Methods

**Animals.** A modified human skeletal $\alpha$-actin promoter (generous gift of Edna C. Hardeman, University of Sydney) was used for all transgenic constructs and allows expression in fast and slow skeletal muscle fiber types without heart expression (40). The Human TRPC3 and dnTRPC6 cDNAs were described previously (41). Four and three lines of TRPC3 and dnTRPC6 TG mouse lines (FVBN background) were generated, respectively, of which one line each was selected based on uniform overexpression in all skeletal muscles examined, without ectopic expression. *Scgd*$^{-/-}$ (C57BL/6 background) mice were provided by Elizabeth M. McNally (University of Chicago). Both male and female littermates were used for analysis of all experiments shown. Female *mdx* mice (C57BL/10 background) were obtained from Jackson Laboratories and crossed with male dnTRPC6 TG mice. Because dystrophin is X-linked, only male mice were used when crossed with the dnTRPC6 TG. All animal experiments were approved by the Institutional Animal Care and Use Committee.

**Western Blotting.** Muscle extracts were prepared by homogenization in cell lysis buffer [20 mM Tris (pH 7.4), 137 mM NaCl, 25 mM $\beta$-glycerophosphate, 2 mM sodium pyrophosphate, 2 mM EDTA, 1 mM sodium orthovanadate, 1% Triton X-100, 10% glycerol, 1 mM phenylmethanesulphonylfluoride, 5 $\mu$g/mL leupeptin, 5 $\mu$g/mL aprotinin and 2 mM benzamide]. Extracts were centrifuged at 13,000 $\times$ *g* for 10 min and 10–30 $\mu$g of protein was separated on a SDS-8% polyacrylamide gel, for subsequent Western blotting by chemiluminescence (Amersham Biosciences). TRPC3 was detected using a rabbit polyclonal antibody from Abcam at a dilution of 1:1000, and TRPC6 antibody was used at 1:1000 (Alomone Labs).

**Immunohistochemistry.** Muscles were excised and snap frozen in Optimal Cutting Temperature (O.C.T., Tissue-Tek) compound. Five-micrometer sections were cut, fixed in 100% ethanol, permeabilized with 0.1% Triton X-100 (Sigma), blocked with 5% BSA, and incubated with primary antibody (1:50 dilution) in a humidified chamber overnight at 4 °C. The dystrophin antibody was a rabbit polyclonal from Santa Cruz Biotechnology, whereas $\alpha$- and $\delta$-sarcoglycan were mouse monoclonal antibodies purchased from Novacastra Laboratories. To visualize each protein an Alexa secondary antibody (Molecular Probes) attached to a fluorophore was used (1:400 dilution).

**Store-Operated Calcium Entry Experiments.** FDB muscles were excised from mice at 6–9 weeks of age and incubated in rodent Ringer's solution with 1 mg/mL collagenase A (Roche) for 60 min at 37 °C. Muscles were washed with Ringer's solution and single fibers were dissociated by triturating with Pasteur pipettes with decreasing bore size. Fibers were then loaded with 5 $\mu$M fura-2 a.m. (Molecular Probes) in Ringer's solution for 45 min at room temperature. Fibers were washed and transferred to a perfusion chamber, excited at 340 nm and 380 nm and emission at 510 nm was measured using a 40$\times$ oil objective and a photomultiplier detection system (Photon Technology International). Fibers were next perfused with calcium-magnesium free Ringer's solution with the myosin ATPase inhibitor BTS (4-Methyl-N-(phenylmethyl)benzenesulfonamide, Tocris Bioscience, 75 $\mu$M) and 200 $\mu$M EGTA (Sigma) for 120 s. This was followed by application of the SERCA inhibitor cyclopiazonic acid (CPA, Fisher, 30 $\mu$M) in the same solution with 10 mM caffeine. Once the 340 nm/380 nm ratio reached a steady state, we perfused fibers with Ringer's with

BTS and recorded the transient increase in SOCE as the 340/380 nm ratio. For each genotype at least four animals were examined, with 5–10 fibers each. Average maximal SOCE was calculated for each genotype and presented as the ΔRatio ($F_{340}/F_{380}$).

**Histological Analyses.** Muscles were paraffin-embedded and sections (5-$\mu$m) were cut at the center of the muscle and stained with either H&E or Masson's trichrome. Between 300–400 fibers were counted for each muscle from every animal. Fiber area was quantified using ImageJ software and broken into ranges. At least 200 fibers were measured for each animal. Fibrosis was quantitated using MetaMorph analysis of blue staining in Masson's trichrome sections.

**Exercise and Evan's Blue Dye Uptake.** To stress the sarcolemma and enhance leakiness, animals were granted access to running wheels for 6 days. On the sixth day mice were injected with Evan's blue dye (EBD), allowed to run overnight, and then killed 16–18 h postinjection. EBD (10 mg/mL) was injected I.P. (0.1 mL/10 g body weight). Quadriceps and gastrocnemius were embedded in O.C.T. and snap-frozen in liquid nitrogen. Sectioning, staining, and viewing were done exactly as described previously (7).

**Affymetrix Microarray Analysis.** mRNA collected from the quadriceps of mice, purified and processed for hybridization on Affymetrix mouse set ST1.0 chips for gene expression profiling as described previously (42).

**Statistical Analysis.** Data are represented as means ± SEM. We used a two-sample Student's *t*-test in situations in which means from two independent groups were compared. A one-way ANOVA was used when comparing means from three or more independent groups, and we applied a Newman-Kuels post hoc test. Values were considered significant when $P < 0.05$.

**ACKNOWLEDGMENTS.** This work was supported by grants from the National Institutes of Health (to J.D.M), the Jain Foundation (to J.D.M), and the Howard Hughes Medical Institute (to J.D.M).

1. Durbeej M, Campbell KP (2002) Muscular dystrophies involving the dystrophin-glycoprotein complex: An overview of current mouse models. *Curr Opin Genet Dev* 12:349–361.
2. Lapidos KA, Kakkar R, McNally EM (2004) The dystrophin glycoprotein complex: Signaling strength and integrity for the sarcolemma. *Circ Res* 94:1023–1031.
3. Blake DJ, Weir A, Newey SE, Davies KE (2002) Function and genetics of dystrophin and dystrophin-related proteins in muscle. *Physiol Rev* 82:291–329.
4. Petrof BJ, Shrager JB, Stedman HH, Kelly AM, Sweeney HL (1993) Dystrophin protects the sarcolemma from stresses developed during muscle contraction. *Proc Natl Acad Sci USA* 90:3710–3714.
5. Turner PR, Fong PY, Denetclaw WF, Steinhardt RA (1991) Increased calcium influx in dystrophic muscle. *J Cell Biol* 115:1701–1712.
6. Turner PR, Westwood T, Regen CM, Steinhardt RA (1988) Increased protein degradation results from elevated free calcium levels found in muscle from mdx mice. *Nature* 335:735–738.
7. Millay DP, et al. (2008) Genetic and pharmacologic inhibition of mitochondrial-dependent necrosis attenuates muscular dystrophy. *Nat Med* 14:442–447.
8. Spencer MJ, Croall DE, Tidball JG (1995) Calpains are activated in necrotic fibers from mdx dystrophic mice. *J Biol Chem* 270:10909–10914.
9. Spencer MJ, Mellgren RL (2002) Overexpression of a calpastatin transgene in mdx muscle reduces dystrophic pathology. *Hum Mol Genet* 11:2645–2655.
10. Gailly P, Boland B, Himpens B, Casteels R, Gillis JM (1993) Critical evaluation of cytosolic calcium determination in resting muscle fibres from normal and dystrophic (mdx) mice. *Cell Calcium* 14:473–483.
11. Han R, Grounds MD, Bakker AJ (2006) Measurement of sub-membrane [Ca2+] in adult myofibers and cytosolic [Ca2+] in myotubes from normal and mdx mice using the Ca2+ indicator FFP-18. *Cell Calcium* 40:299–307.
12. Head SI (1993) Membrane potential, resting calcium, and calcium transients in isolated muscle fibres from normal and dystrophic mice. *J Physiol* 469:11–19.
13. Mallouk N, Jacquemond V, Allard B (2000) Elevated subsarcolemmal Ca2+ in mdx mouse skeletal muscle fibers detected with Ca2+-activated K+ channels. *Proc Natl Acad Sci USA* 97:4950–4955.
14. Pressmar J, Brinkmeier H, Seewald MJ, Naumann T, Rudel R (1994) Intracellular Ca2+ concentrations are not elevated in resting cultured muscle from Duchenne (DMD) patients and in MDX mouse muscle fibres. *Pflugers Arch* 426:499–505.
15. Boittin FX, et al. (2006) Ca2+-independent phospholipase A2 enhances store-operated Ca2+ entry in dystrophic skeletal muscle fibers. *J Cell Sci* 119:3733–3742.
16. Fong PY, Turner PR, Denetclaw WF, Steinhardt RA (1990) Increased activity of calcium leak channels in myotubes of Duchenne human and mdx mouse origin. *Science* 250:673–676.
17. Franco A, Jr, Lansman JB (1990) Calcium entry through stretch-inactivated ion channels in mdx myotubes. *Nature* 344:670–673.
18. Vandebrouck C, Martin D, Colson-Van Schoor M, Debaix H, Gailly P (2002) Involvement of TRPC in the abnormal calcium influx observed in dystrophic (mdx) mouse skeletal muscle fibers. *J Cell Biol* 158:1089–1096.
19. Allen DG, Whitehead NP, Yeung EW (2005) Mechanisms of stretch-induced muscle damage in normal and dystrophic muscle: Role of ionic changes. *J Physiol* 567:723–735.
20. Vandebrouck A, et al. (2007) Regulation of capacitative calcium entries by alpha1-syntrophin: Association of TRPC1 with dystrophin complex and the PDZ domain of alpha1-syntrophin. *Faseb J* 21:608–617.
21. Yeung EW, et al. (2005) Effects of stretch-activated channel blockers on [Ca2+]i and muscle damage in the mdx mouse. *J Physiol* 562:367–380.
22. Collet C, Allard B, Tourneur Y, Jacquemond V (1999) Intracellular calcium signals measured with indo-1 in isolated skeletal muscle fibres from control and mdx mice. *J Physiol 520 Pt* 2:417–429.
23. Moens P, Baatsen PH, Marechal G (1993) Increased susceptibility of EDL muscles from mdx mice to damage induced by contractions with stretch. *J Muscle Res Cell Motil* 14:446–451.
24. McArdle A, Edwards RH, Jackson MJ (1994) Time course of changes in plasma membrane permeability in the dystrophin-deficient mdx mouse. *Muscle Nerve* 17:1378–1384.
25. Bansal D, et al. (2003) Defective membrane repair in dysferlin-deficient muscular dystrophy. *Nature* 423:168–172.
26. Bashir R, et al. (1998) A gene related to Caenorhabditis elegans spermatogenesis factor fer-1 is mutated in limb-girdle muscular dystrophy type 2B. *Nat Genet* 20:37–42.
27. Liu J, et al. (1998) Dysferlin, a novel skeletal muscle gene, is mutated in Miyoshi myopathy and limb girdle muscular dystrophy. *Nat Genet* 20:31–36.
28. Collet C, Ma J (2004) Calcium-dependent facilitation and graded deactivation of store-operated calcium entry in fetal skeletal muscle. *Biophys J* 87:268–275.
29. Gutierrez-Martin Y, Martin-Romero FJ, Henao F (2005) Store-operated calcium entry in differentiated C2C12 skeletal muscle cells. *Biochim Biophys Acta* 1711:33–40.
30. Maroto R, et al. (2005) TRPC1 forms the stretch-activated cation channel in vertebrate cells. *Nat Cell Biol* 7:179–185.
31. Weigl L, Zidar A, Gscheidlinger R, Karel A, Hohenegger M (2003) Store operated Ca2+ influx by selective depletion of ryanodine sensitive Ca2+ pools in primary human skeletal muscle cells. *Naunyn Schmiedebergs Arch Pharmacol* 367:353–363.
32. Ambudkar IS, Ong HL, Liu X, Bandyopadhyay BC, Cheng KT (2007) TRPC1: The link between functionally distinct store-operated calcium channels. *Cell Calcium* 42:213–223.
33. Gervasio OL, Whitehead NP, Yeung EW, Phillips WD, Allen DG (2008) TRPC1 binds to caveolin-3 and is regulated by Src kinase - role in Duchenne muscular dystrophy. *J Cell Sci* 121:2246–2255.
34. Whitehead NP, Yeung EW, Allen DG (2006) Muscle damage in mdx (dystrophic) mice: Role of calcium and reactive oxygen species. *Clin Exp Pharmacol Physiol* 33:657–662.
35. Iwata Y, Katanosaka Y, Arai Y, Shigekawa M, Wakabayashi S (2009) Dominant-negative inhibition of Ca2+ influx via TRPV2 ameliorates muscular dystrophy in animal models. *Hum Mol Genet* 18:824–834.
36. Dunn JF, Bannister N, Kemp GJ, Publicover SJ (1993) Sodium is elevated in mdx muscles: Ionic interactions in dystrophic cells. *J Neurol Sci* 114:76–80.
37. Sokolow S, et al. (2004) Impaired neuromuscular transmission and skeletal muscle fiber necrosis in mice lacking Na/Ca exchanger 3. *J Clin Invest* 113:265–273.
38. Deval E, et al. (2002) Na(+)/Ca(2+) exchange in human myotubes: Intracellular calcium rises in response to external sodium depletion are enhanced in DMD. *Neuromuscul Disord* 12:665–673.
39. Hirn C, Shapovalov G, Petermann O, Roulet E, Ruegg UT (2008) Nav1.4 deregulation in dystrophic skeletal muscle leads to Na+ overload and enhanced cell death. *J Gen Physiol* 132:199–208.
40. Brennan KJ, Hardeman EC (1993) Quantitative analysis of the human alpha-skeletal actin gene in transgenic mice. *J Biol Chem* 268:719–725.
41. Hofmann T, Schaefer M, Schultz G, Gudermann T (2002) Subunit composition of mammalian transient receptor potential channels in living cells. *Proc Natl Acad Sci USA* 99:7461–7466.
42. Oka T, et al. (2006) Cardiac-specific deletion of Gata4 reveals its requirement for hypertrophy, compensation, and myocyte viability. *Circ Res* 98:837–845.